Opposing functions of two sub-domains of the SNARE-complex in neurotransmission

Jens P Weber[1], Kerstin Reim[2] and Jakob B Sørensen[1,3,*]

[1]Molecular Mechanisms of Exocytosis, Max-Planck-Institute for Biophysical Chemistry, Göttingen, Germany, [2]Department of Molecular Neurobiology and Center for Molecular Physiology of the Brain, Max Planck Institute of Experimental Medicine, Göttingen, Germany and [3]Neurosecretion Group, Department of Neuroscience and Pharmacology, Faculty of Health Sciences, University of Copenhagen, Copenhagen N, Denmark

The SNARE-complex consisting of synaptobrevin-2/VAMP-2, SNAP-25 and syntaxin-1 is essential for evoked neurotransmission and also involved in spontaneous release. Here, we used cultured autaptic hippocampal neurons from *Snap-25* null mice rescued with mutants challenging the C-terminal, N-terminal and middle domains of the SNARE-bundle to dissect out the involvement of these domains in neurotransmission. We report that the stabilities of two different sub-domains of the SNARE-bundle have opposing functions in setting the probability for both spontaneous and evoked neurotransmission. Destabilizing the C-terminal end of the SNARE-bundle abolishes spontaneous neurotransmitter release and reduces evoked release probability, indicating that the C-terminal end promotes both modes of release. In contrast, destabilizing the middle or deleting the N-terminal end of the SNARE-bundle increases both spontaneous and evoked release probabilities. In both cases, spontaneous release was affected more than evoked neurotransmission. In addition, the N-terminal deletion delays vesicle priming after a high-frequency train. We propose that the stability of N-terminal two-thirds of the SNARE-bundle has a function for vesicle priming and limiting spontaneous release.

Introduction

Synaptic transmission depends on the exquisite timing of the fusion of synaptic vesicles with the presynaptic plasma membrane. To explain the speed and fidelity of synaptic transmission, early studies invoked a special sub-pool of neurotransmitter, today known as the readily releasable pool (RRP) of vesicles, from which release occurs rapidly when triggered by an action potential (Birks and Macintosh, 1957). This idea implies that vesicles undergo a maturation step before they become releasable. This so-called priming process pushes the vesicle closer to being released, but at the same time prevents release from taking place spontaneously. Thus, already the simplest model of synaptic transmission implies that in a certain sense the fusion machinery must be both stimulatory and inhibitory (Sorensen, 2004).

Recent studies have identified the molecular components of the vesicular release machinery. Central for evoked neurotransmission is the SNARE-complex, an extended four-helical parallel bundle (Sutton *et al*, 1998) consisting of SNARE-motifs from three proteins: synaptobrevin-2 (VAMP-2) (Baumert *et al*, 1989; Elferink *et al*, 1989), which is anchored in the vesicular membrane (v-SNARE), and syntaxin-1 (Bennett *et al*, 1992) and SNAP-25 (Oyler *et al*, 1989), which are plasma membrane proteins (t-SNAREs) (Jahn and Scheller, 2006). By forming a ternary complex, the SNARE-proteins bridge the membranes, and it is hypothesized that the remarkable stability of the complex has a decisive function in overcoming the energy barrier for fusion (Jahn and Scheller, 2006). During assembly, the SNARE-complex is oriented with its C-terminal end pointing towards the nascent fusion pore and the N-terminal end pointing away from it (Hanson *et al*, 1997; Sutton *et al*, 1998). Recent investigations have focused on delineating the assembly pathway of the SNARE-complex, and its involvement in different steps in the exocytotic cascade. In chromaffin cells, both SNAP-25 and syntaxin are involved in docking vesicles to the plasma membrane, probably by binding to vesicular synaptotagmin-1 (de Wit *et al*, 2009), the calcium sensor for exocytosis. The function of Munc18-1, also a docking factor in chromaffin cells (Voets *et al*, 2001), seems to be to stabilize 1:1 SNAP-25:syntaxin complexes and assist assembly of synaptobrevin to this acceptor complex (Shen *et al*, 2007), which drives vesicle priming (Deak *et al*, 2009). In mutagenesis studies carried out in chromaffin cells, we provided evidence for a two-step assembly process of the SNARE-complex, in which the N-terminal end of synaptobrevin associates to the SNAP-25:syntaxin acceptor complex during vesicle priming, and C-terminal assembly of the complex coincides with calcium influx and drives membrane fusion (Sorensen *et al*, 2006; Walter *et al*, 2010), resembling the closing of a zipper.

The SNARE-complex is involved in both evoked and spontaneous neurotransmission. However, removal of a SNARE-component typically eliminates evoked release, whereas spontaneous release persists at a reduced rate, indicating that the requirements for spontaneous release are less strict (Deitcher *et al*, 1998; Schoch *et al*, 2001; Washbourne *et al*, 2002; Bronk *et al*, 2007; Delgado-Martinez *et al*, 2007). These and other observations led to the idea that spontaneous release might occur from a specific set of vesicles, require an alternative fusion complex or a SNARE-complex formed with lower stringency (Glitsch, 2008; Wasser and Kavalali, 2009). Data obtained after genetic

*Corresponding author. Department of Neuroscience and Pharmacology, Faculty of Health Sciences, University of Copenhagen, Blegdamsvej 3C, 2200 Copenhagen N, Denmark. Tel.: +45 3532 7931; Fax: +45 3532 7644; E-mail: jakobbs@sund.ku.dk

elimination of synaptotagmin-1 implicates this protein in both evoked and spontaneous release modes (Rizo and Rosenmund, 2008; Sudhof and Rothman, 2009). Another protein interacting with the SNARE-complex is complexin, which has also been shown to both clamp spontaneous release events and modulate the release probability of evoked release (Rizo and Rosenmund, 2008; Sudhof and Rothman, 2009). Both complexin and synaptotagmin interact directly with the SNARE-complex in different states of assembly. However, also Munc13-1, a priming protein, which is assumed to assist in SNARE-complex assembly and thus act upstream of synaptotagmin/complexin, has been shown to modulate spontaneous release events (Basu *et al*, 2007; Lou *et al*, 2008). Thus, both proteins upstream and downstream of SNARE-complex assembly affect spontaneous release.

Here, we set out to understand the effect of sequential SNARE-complex assembly on synaptic transmission. On the basis of our earlier studies in chromaffin cells, we hypothesized that the N- and C-terminal ends of the complex are differentially involved in short-term synaptic plasticity, spontaneous release and recovery after strong stimulation. Although these expectations were borne out by experiments, we also find that the two ends of the SNARE-complex have partly opposing functions in neurotransmission. Whereas C-terminal mutations designed to destabilize the SNARE-complex led to a decrease in vesicular release probability and spontaneous release, more N-terminal mutations increased both quantities. These findings show that the SNARE-complex—quite likely in conjunction with external factors such as complexin—harbours both the inhibitory and the stimulatory functions, which are a necessary prerequisite for fast neurotransmission.

Results

### Introduction of SNAP-25 mutations into hippocampal neurons

To understand the function of the SNARE-complex in evoked and spontaneous synaptic transmission, we introduced

mutations in SNAP-25 along the SNARE-motif (Figure 1) and expressed the mutants in hippocampal cultures using recombinant lentiviruses. The mutations were alanine substitutions of 'layer' residues, which face the centre of the complex (Fasshauer *et al*, 1998), in addition to a C-terminal deletion of 9 amino acids (CΔ9), which corresponds to cleavage by Botulinum Neurotoxin A (BoNT/A), and a 24 amino-acid N-terminal deletion (NΔ24), which had not been studied before. All constructs were N-terminally fused to EGFP, which does not affect the function of wild-type SNAP-25, as shown by comparing rescue experiments presented below to earlier data (Delgado-Martinez *et al*, 2007). The mutants were all expressed using pseudotyped lentiviruses infecting hippocampal neurons. We estimated the overexpression level of our mutants by western blotting. The exogeneous EGFP-SNAP-25 was recognized by its higher molecular weight and the expression level estimated by normalization to endogenous SNAP-25. Wild-type SNAP-25 (formally: EGFP-SNAP-25) was overexpressed 2.1-fold over endogenous levels, and most mutations were expressed to similar extents (overexpression levels ranging from 1.0 to 3.9-fold for different constructs). An exception was NΔ24, which was only expressed 0.4-fold (Supplementary Figure 1).

The SNARE-complexes formed *in vitro* were earlier reported to be only slightly destabilized by these mutations (Sorensen *et al*, 2006). To investigate the properties of SNARE-complexes in cells, we performed a pull-down assay with glutathione *S*-transferase (GST) complexin-1. Complexin-1 binds to assembled ternary SNARE-complexes (Chen *et al*, 2002; Pabst *et al*, 2002). As a control, we used mutated complexin-1 (K69A/Y70A), which cannot bind (Xue *et al*, 2007). All mutants studied here were able to form ternary complexes, which bound specifically to complexin-1 (Supplementary Figure 1). This shows that the EGFP-tag does not interfere with SNARE-complex formation or binding to auxiliary proteins. Overall, our expression system results in mild overexpression and the mutations do not radically change overall properties of the SNARE-complex either *in vitro* or *in vivo*.
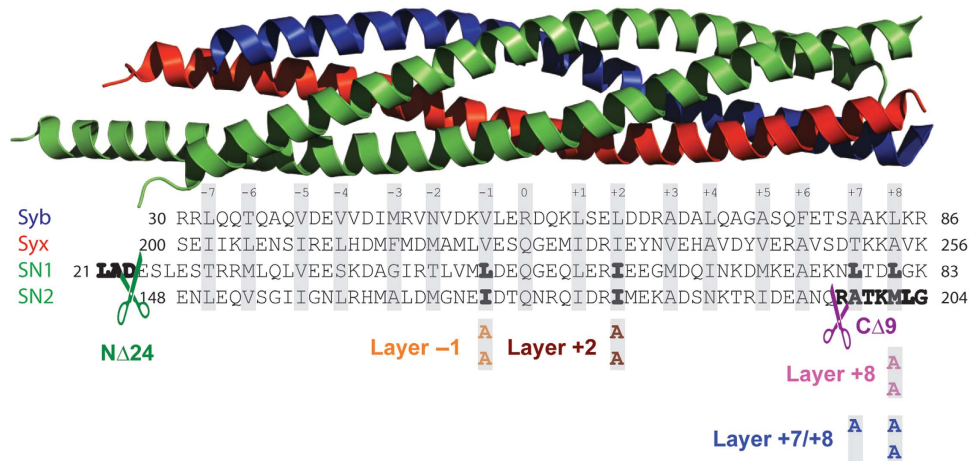
Figure 1 Structure of the SNARE-complex and the introduced mutations. Top: Crystal structure of the SNARE-complex (Sutton *et al*, 1998) rendered by PyMOL; SNAP-25 (green), Syntaxin-1 (red) and Synaptobrevin-2 (blue). Bottom: wild-type sequences of the SNAREs approximately aligned with the structure above. Layers are indicated by grey bars. Layer residues that were mutated to alanines are highlighted in bold and the mutated sequence shown below in the colour coding used throughout the figures. N- and C-terminal deletions in the first (SN1) and second (SN2) SNARE-motif of SNAP-25 are indicated by scissors.
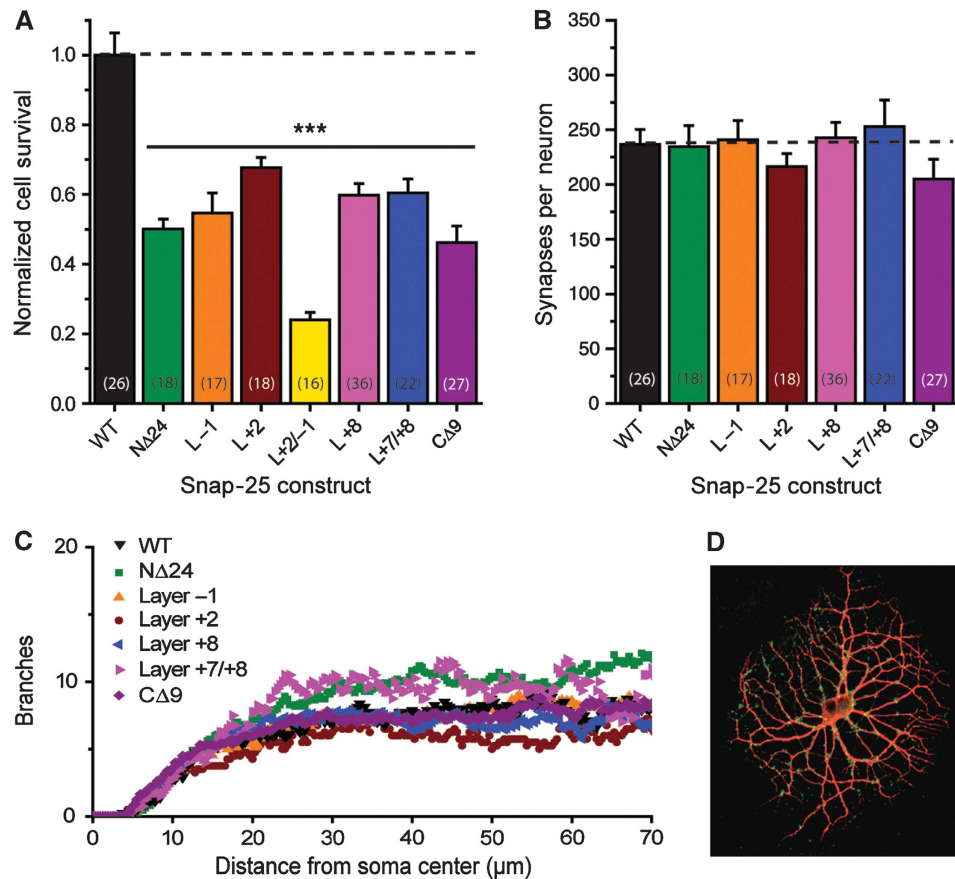
Figure 2 Rescue of neuronal survival, synaptogenesis and branching. (**A**) Survival of *Snap-25* null neurons expressing different constructs by lentiviral transduction. WT indicates the EGFP-SNAP-25 fusion protein. Mutants are colour coded (see Figure 1). All constructs led to sub-optimal survival compared with WT (one-way ANOVA, ***$P < 0.001$), but nevertheless substantial rescue compared with non-expressing *Snap-25* null (1.3% survival; Delgado-Martinez *et al*, 2007). (**B**) Number of synapses per autaptic neuron as assessed by synaptobrevin staining. No difference between constructs could be identified (one-way ANOVA, $P > 0.499$). (**C**) Dendritic branching index as function of distance from soma centre as assessed by MAP-2 staining followed by automatic branch detection (Delgado-Martinez *et al*, 2007). No systematic difference between constructs could be identified. (**D**) Example of MAP-2 and synaptobrevin-2 double-stained neuron (red channel: MAP-2; green channel: synaptobrevin-2).

Survival and branching of rescued neurons

We next expressed the mutants in hippocampal neurons from *Snap-25* null mice. Knockout of SNAP-25 leads to lower neuronal survival *in vitro* and decreased dendritic branching and synapse numbers (Delgado-Martinez *et al*, 2007). We, therefore, tested those parameters for the mutants investigated here (Figure 2). All constructs significantly rescued survival (Figure 2A), however, not to control values (EGFP-SNAP-25 rescue), indicating that the integrity of the entire SNARE-motif is needed for maximal neuronal survival. The effect of mutation seemed additive; a combined Layer −1 and Layer +2 mutation (a quadrupel alanine substitution) supported even less survival than both single-layer mutants. As survival is much lower in the low-density autaptic configuration used for electrophysiology, this mutation could not be studied any further. All constructs resulted in similar synapse counts in surviving neurons (Figure 2B and D) (one-way ANOVA, $P > 0.499$). Branching was assessed by MAP-2 staining and automatic branch detection (Delgado-Martinez *et al*, 2007) (Figure 2C). The constructs investigated here resulted in branching indistinguishable from wild-type rescue, in contrast to the impaired branching earlier described in *Snap-25* null cells (Delgado-Martinez *et al*, 2007). Finally,

we investigated the localization of expressed EGFP-SNAP-25. All SNAP-25 constructs were distributed throughout the neurites and did not seem restricted to presynaptic boutons, in agreement with earlier data (Grosse *et al*, 1999; Verderio *et al*, 2004; Tafoya *et al*, 2006; Delgado-Martinez *et al*, 2007). Nevertheless, the signal from SNAP-25 overlapped with the synaptic marker synaptobrevin-2 (Supplementary Figure 2).

In conclusion, the SNAP-25 mutants used here led to moderately decreased rescue of neuronal survival, but they seemed normally distributed in the cell and supported normal branching and synapse numbers in surviving neurons.

C-terminal mutations: arrest of spontaneous release

The mutants were expressed in *Snap-25* null glutamatergic hippocampal neurons forming autapses *in vitro* (Bekkers and Stevens, 1991) and synaptic transmission monitored by patch-clamp electrophysiology. As control experiment, we used null neurons rescued with EGFP-SNAP-25 (denoted 'WT' in the figures). The result of C-terminal mutation is shown in Figure 3. These mutations destabilize the C-terminal end of the SNARE-complex, but they do still allow SNARE-complex assembly (Sorensen *et al*, 2006). The EPSC amplitude was normal in the Layer +8 mutant (a double
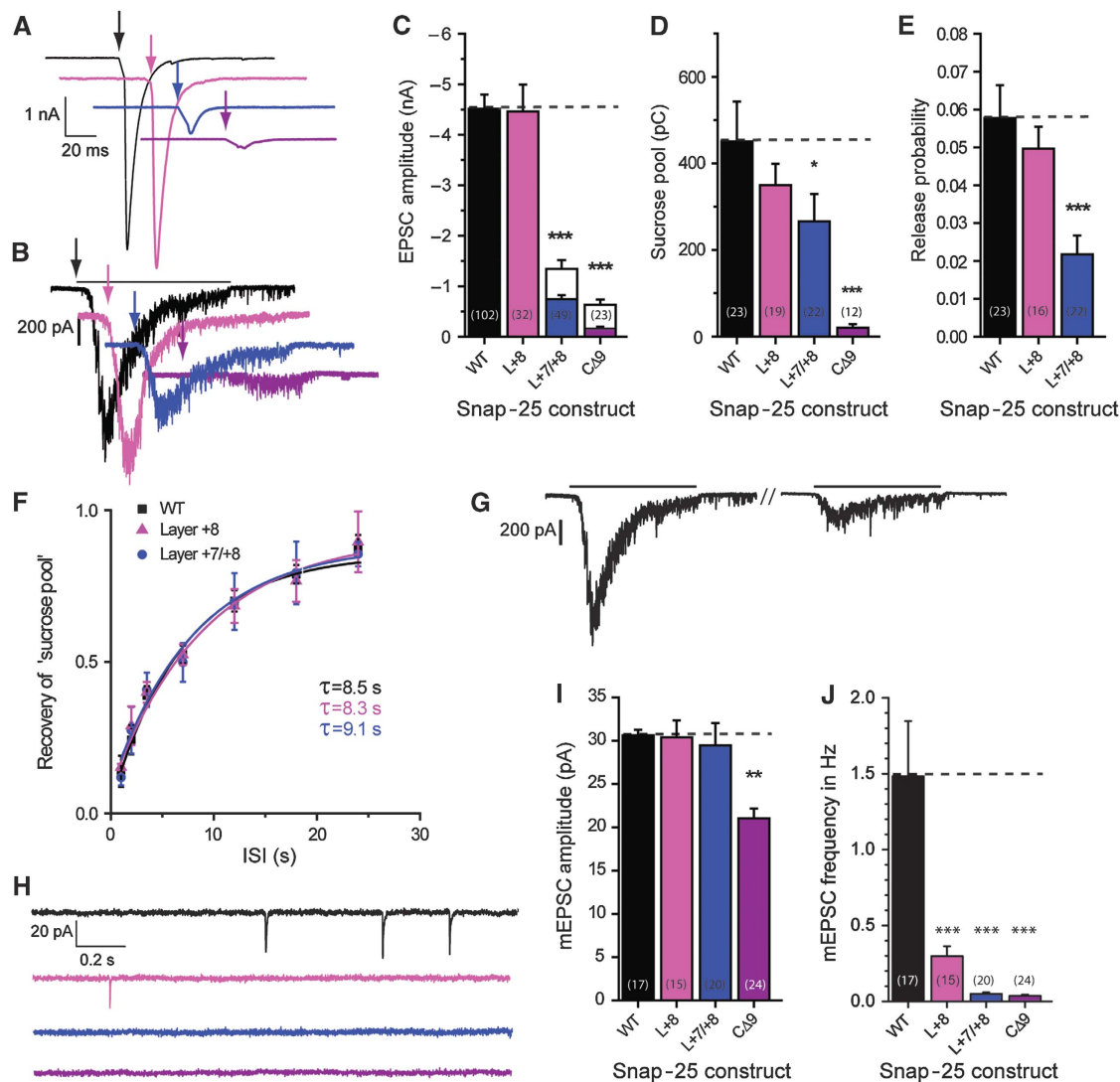
Figure 3 C-terminal mutations impair evoked and abolish spontaneous release. (**A**) Example EPSC traces; arrows indicate time of stimulation. Colour coding of mutations according to Figure 1. (**B**) Example sucrose traces; black line indicates time of exposure for WT trace (black) and arrows begin of exposure. (**C**) EPSC amplitudes (mean ± s.e.m.). Stacked bars indicate naive EPSC amplitudes (coloured) and maximal facilitated amplitudes (see also below). Inserted numbers in parenthesis indicate number of cells (*n*) in each group. The Layer $+7/+8$ mutation (a triple alanine substitution in layers $+7$ and $+8$) and the C$\Delta9$ deletion caused highly significant decreases in EPSC amplitudes. (**D**) Sucrose pool sizes in pC (mean ± s.e.m.) were progressively decreased by C-terminal mutation. (**E**) Release probabilites (mean ± s.e.m.) derived by dividing EPSC charge by the sucrose pool estimated in the same neuron were significantly decreased in the Layer $+7/+8$ mutation. (**F**) Recovery of the sucrose pool after depletion. Lines are fit of an exponential recovery function ($y = 1 - e^{-t/\tau}$). ISI, inter-stimulus interval. No change in the recovery of the sucrose pool was identified on C-terminal mutation. (**G**) Example WT traces of sucrose recovery, depleting pulse and test pulse. (**H**) Example spontaneous mEPSC traces in the presence of tetrodotoxin (TTX). (**I**) mEPSC amplitudes (mean ± s.e.m.). The C$\Delta9$ deletion led to a decrease in mEPSC amplitude. (**J**) mEPSC frequencies (mean ± s.e.m.) were progressively depressed by C-terminal mutation. Note that the depression was even more dramatic than the inhibition of evoked EPSCs (**C**) (*$P < 0.05$; **$P < 0.01$; ***$P < 0.001$).

alanine substitution), severely inhibited in the Layer $+7/+8$ mutant (a triple alanine substitution) and nearly abolished in the C$\Delta9$ (Figure 3A and C). Thus, EPSC amplitude was reduced according to mutation severity. We next stimulated neurotransmission by application of hyperosmotic sucrose, which releases the 'RRP' (RRP$_{suc}$) of synaptic vesicles (Rosenmund and Stevens, 1996). The response was again inhibited according to mutation severity (Figure 3B and D). Dividing the EPSC charge by the charge released by sucrose gives the probability of releasing an RRP$_{suc}$ vesicle by an action potential. This number was significantly decreased for the Layer $+7/+8$ mutation (Figure 3E) indicating that evoked release is affected more by this mutation than

sucrose-stimulated release. For the C$\Delta9$ mutant, the release probability was not calculated, because it would involve dividing two near-zero values with each other. The ability of synapses to refill their stores of releasable vesicles was studied by applying two sucrose stimulations at variable interstimulus intervals (Figure 3G). Refilling occurred with a time constant ~8 s, which is in good agreement with earlier publications (Rosenmund and Stevens, 1996; Stevens and Wesseling, 1998) and remained unchanged after C-terminal mutation (Figure 3F).

The C-terminal mutations had a striking effect on spontaneous release events: the Layer $+8$ mutation decreased the mini-frequency to 20% of control values, whereas with Layer

$+7/+8$ and CΔ9, mEPSCs were almost abolished (3.3 and 2.4% of control frequencies, respectively; Figure 3H and J). With the CΔ9, the mEPSC amplitude was significantly decreased (Figure 3I), probably indicating that this mutation affected the density or clustering of postsynaptic receptors. A function for SNAP-25 in kainate and NMDA receptor trafficking has been described earlier (Lan *et al*, 2001; Selak *et al*, 2009).

In conclusion, mutation in the C-terminal end of the SNARE-motif of SNAP-25 leads to decreased EPSC and 'sucrose pool' sizes, whereas abolishing spontaneous release. These data contrast with the finding of decreased evoked release and persisting spontaneous release in SNAP-25 knockouts (Washbourne *et al*, 2002; Bronk *et al*, 2007; Delgado-Martinez *et al*, 2007).

Mutations in the middle: unclamping spontaneous release

Two double alanine substitutions around the middle of the SNARE-motif (in Layer -1 and Layer $+2$; Figure 1) were studied here. Both mutations left EPSC amplitude and sucrose response unaltered (Figure 4A–D). Consequently, also the release probability of RRP$_{suc}$ vesicles was normal (Figure 4E). Recovery of the sucrose pool proceeded at a rate indistinguishable from wild type (Figure 4F). Recovery of the EPSC was studied by emptying the pool of ready-releasable vesicles using a train of 100 APs at 40 Hz (see also below and Figure 7), followed by a single test stimulus presented after a variable interstimulus interval (Figure 4G). Recovery proceeded with a time constant of $\sim$1.8 s, which was not changed by mutation (Figure 4H). These data indicate that refilling of the RRP is faster after a high-frequency train, as reported earlier (Stevens and Wesseling, 1998; Wang and Kaczmarek, 1998). Overall, the data indicate no major problems with these mutants in evoked or sucrose-stimulated release.

Both mutations led to a four- to five-fold increase in minirate (Figure 4I and K), whereas the mEPSC amplitude was unchanged (Figure 4J). Thus, mutation in the middle of the complex leaves EPSC size unchanged, but unclamps spontaneous release, whereas C-terminal mutation inhibits EPSC size and abolishes spontaneous release. This finding might have two explanations: if SNAP-25 competes with other Qb/Qc-SNAREs (such as SNAP-29 (Steegmaier *et al*, 1998) or SNAP-47 (Holt *et al*, 2006)) in the cell, mutating the N-terminal end, which probably initiates assembly (Fasshauer and Margittai, 2004), might cause SNAP-25 to 'lose' this competition, favouring neurotransmitter release driven by syntaxin binding to the other homologues, which might be more prone to spontaneous release. Another possibility is that the neuronal SNARE-complex itself has changed properties to support spontaneous release. When combining a mutation in the middle (Layer -1) with the C-terminal triple mutation (Layer $+7/+8$), the C-terminal deletion dominated the phenotype of the combined (Layer $-1/+7/+8$) mutant and almost eliminated EPSCs (Figure 4A and C) and mEPSCs (Figure 4K), confirming that competition is not the reason for the phenotype. Thus, on mutation in the middle, the SNARE-complex supports spontaneous release at a higher rate, and this mode of release still depends on the C-terminal end of the SNARE-complex.

N-terminal deletion: unclamping spontaneous release and delaying recovery

We next tested the effect of deleting 24 amino acids from the N-terminal end of SNAP-25. The crystal structure of the SNARE-complex indicates that the first layer (Layer -7) starts just C-terminal of amino-acid 24 (Figure 1); however, deleting the first amino acids might still be expected to destabilize this end of the complex and interfere with N-terminal assembly of the ternary (synaptobrevin:syntaxin:SNAP-25) or possibly the binary (SNAP-25:syntaxin) SNARE-complex (Fasshauer and Margittai, 2004; Walter *et al*, 2010). At the same time, uncharacterized structural features located N-terminal to the resolved crystal structure will be lost.

Snap-25 null neurons rescued with the NΔ24 mutant displayed normal EPSC amplitudes (Figure 5A and C), sucrose pools (Figure 5B and D) and release probabilities of the sucrose pool (Figure 5E). Recovery of the sucrose pool was also unchanged (Figure 5F), but recovery after a train of 100 action potentials (40 Hz) was now markedly delayed (Figure 5G) and proceeded in an exponential manner with a time constant of $\sim$7.1 s instead of the $\sim$1.8 s found in the wild-type case.

Spontaneous release was also changed with the NΔ24 mutant; the frequency was increased by a factor $\sim$4 (Figure 5H and J), whereas mEPSC amplitudes were unchanged (Figure 5I) compared with controls. Thus, this mutation displays a change in spontaneous release, which is similar to mutations around the middle of the complex.

Thus, the N-terminal deletion of SNAP-25 fails specifically in clamping release before the arrival of an AP and in the recruitment after a train of action potentials.

Bidirectional changes in short-term synaptic plasticity and release probability

In the next three sets of experiments, we investigated synaptic transmission in rescued hippocampal neurons during repetitive stimulation.

We first applied trains of five APs at either 1 or 50 Hz frequencies. In the wild-type case, EPSC amplitudes depressed during both 50-Hz (Figure 6A–C) and 1-Hz stimulation (Supplementary Figure 3). C-terminal mutations resulted in a shift towards facilitation, which was most pronounced at 50 Hz, in which the buildup of the intracellular calcium concentration is stronger (Figure 6A; Supplementary Figure 3). We thus hypothesized that C-terminal mutations displayed a shift in the calcium dependence of release. This expectation was confirmed by experiments varying the external $[Ca^{2+}]$ (Supplementary Figure 4). The calcium dependence for the CΔ9 was displaced far towards larger $[Ca^{2+}]$, whereas the Layer $+8$ and Layer $+7/+8$ displayed intermediate phenotypes (Supplementary Figure 4). The Layer -1, Layer $+2$ and the NΔ24 deletion all displayed mild changes towards short-term synaptic depression during both types of trains (Figure 6B and C; Supplementary Figure 3), that is in the opposite direction as the C-terminal mutations.

The data on short trains led us to test whether the synaptic release probability was changed by our mutations. A changed release probability could change the depletion of vesicles, and thereby cause the observed short-term synaptic plasticity phenotypes (Zucker and Regehr, 2002). The rundown of NMDA-driven EPSCs in the presence of the near-irreversible
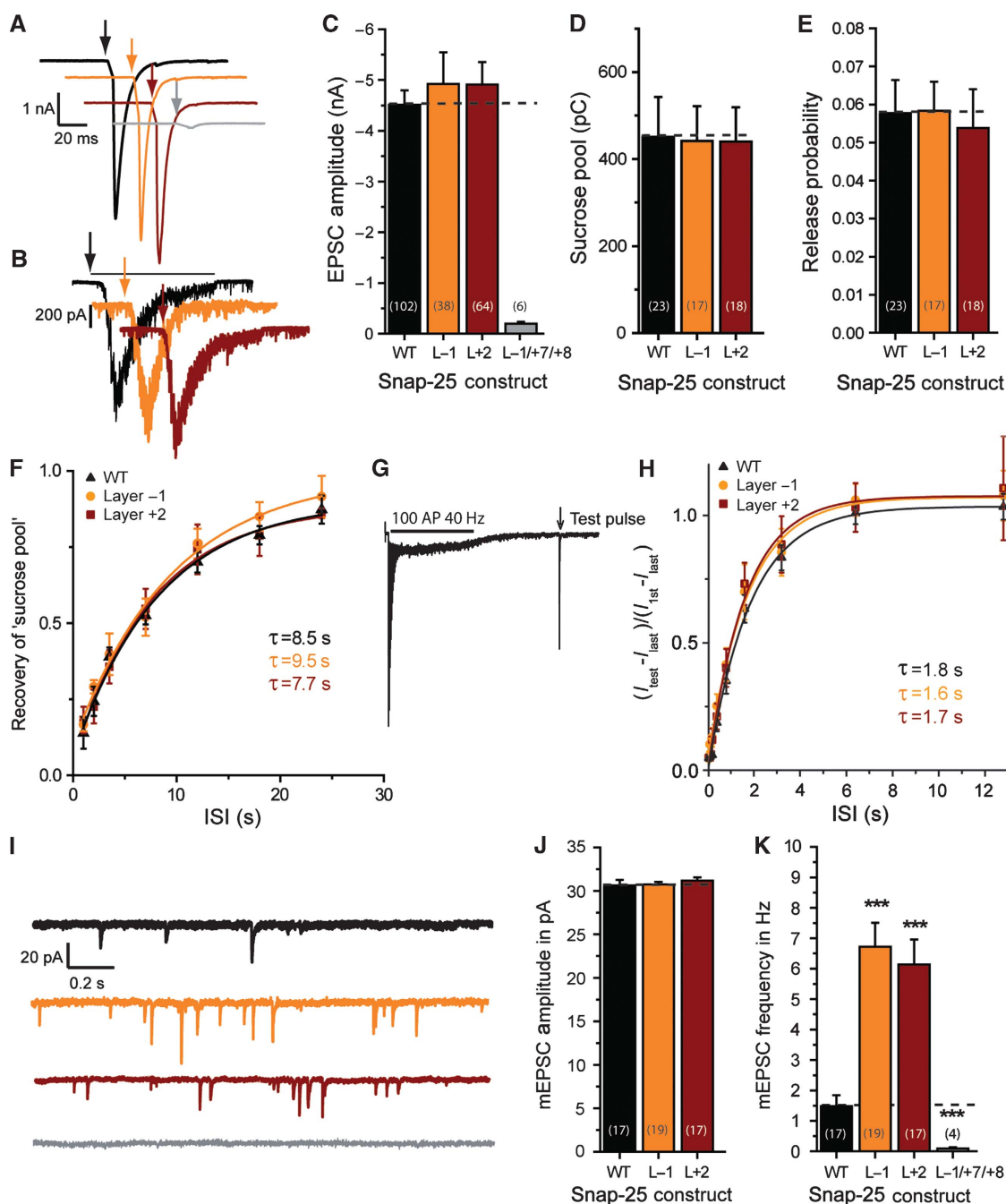
Figure 4 Mutations in the middle of the SNARE-complex increase spontaneous release. (**A**) Example EPSC traces; arrows indicate time of stimulation. Colour coding of mutations according to Figure 1. (**B**) Example sucrose traces; black line indicates time of exposure for WT example and arrows begin of exposure. (**C**) EPSC amplitudes (mean ± s.e.m.) were not significantly changed by middle mutations. (**D**) Sucrose pool sizes in pC (mean ± s.e.m.) remained unchanged after mutation. (**E**) Release probabilites (mean ± s.e.m.) derived from EPSC and sucrose pool estimates remained unchanged. (**F**) Recovery of the sucrose pool after depletion remained unchanged by mutation. (**G**) Example of a pool depleting train (100AP @ 40 Hz) with a single test pulse to probe recovery after depletion (WT trace). Stimulus artefacts have been blanked. (**H**) Recovery after train depletion. The quantity plotted is the amplitude of the test pulse (I_{test}) minus the amplitude of the last train EPSC (I_{last}), divided by the amplitude of the first train EPSC (I_{1st}) minus the amplitude of the last train EPSC (I_{last}). This is the recovery of the component, which disappears during a train. (**I**) Example spontaneous mEPSC traces in the presence of TTX. (**J**) mEPSC amplitudes (mean ± s.e.m.). (**K**) mEPSC frequencies (mean ± s.e.m.) were increased for the Layer $+1$ and Layer $+2$ mutations, but almost abolished when the Layer -1 mutation was combined with the triple mutation in Layers $+7$ and $+8$ (L$-1/+7/+8$) (***$P < 0.001$).

blocker MK801 yields information about the probability that a synapse releases a quantum during stimulation (Hessler et al, 1993; Rosenmund et al, 1993). Our data (Figure 6D–G) show double exponential decays, consistent with heterogeneity of synaptic release probabilities (Hessler et al, 1993;

Rosenmund et al, 1993). Overall, N-terminal and middle mutations led to an increase in synaptic release probability (i.e. faster rundown with MK801) (Figure 6F and G), whereas with the C-terminal mutations, the synaptic release probability was decreased (i.e. slower rundown;
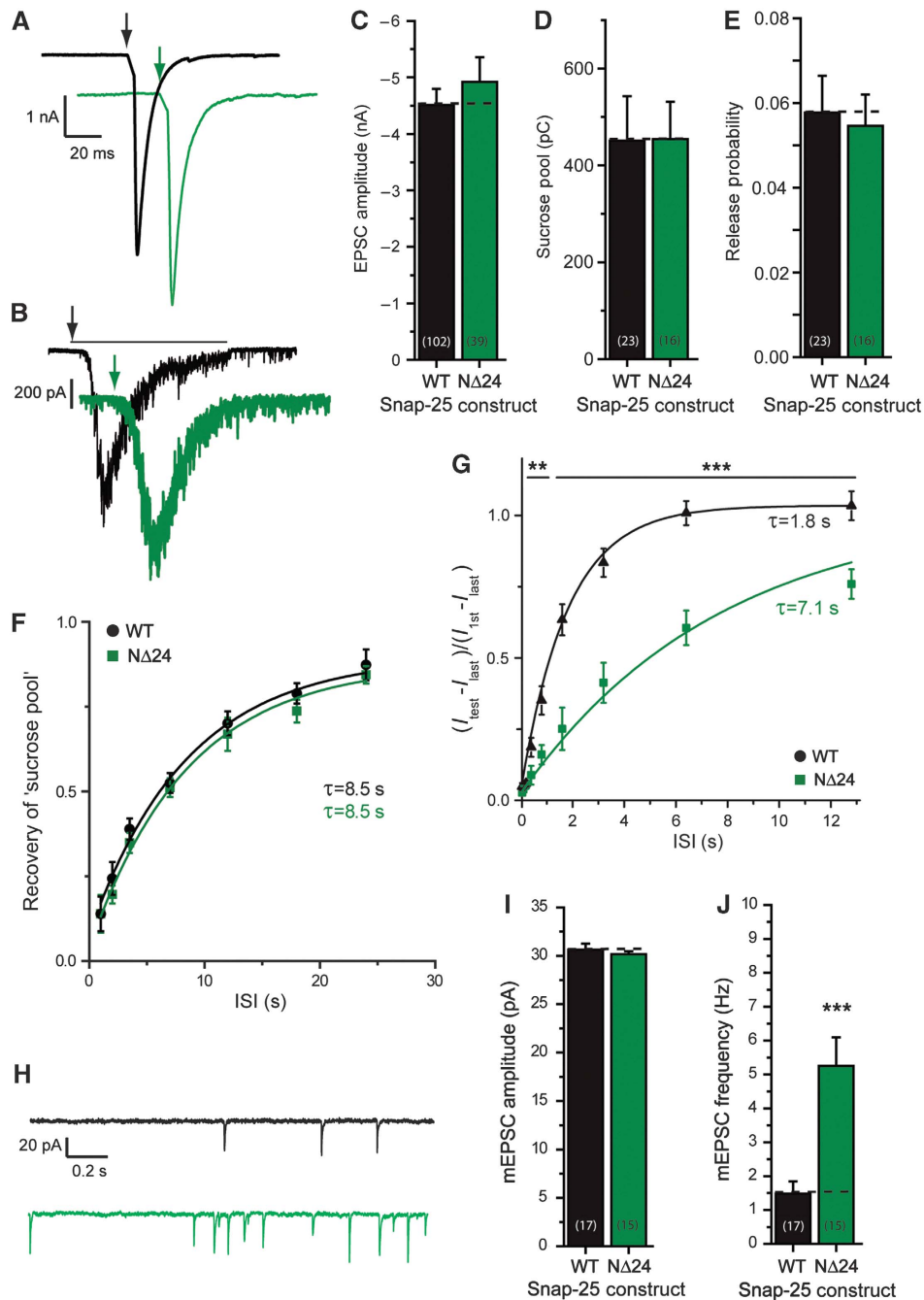
Figure 5 N-terminal deletion impairs recovery of EPSCs after depletion and increases spontaneous release. (**A**) Example EPSC traces; arrows indicate time of stimulation. Colour coding of mutation according to Figure 1. (**B**) Example sucrose traces; black line indicates time of exposure for WT example and arrows begin of exposure. (**C**) EPSC amplitudes (mean ± s.e.m.) were not significantly changed in the NΔ24 deletion. (**D**) Sucrose pool sizes in pC (mean ± s.e.m.) remained unchanged after N-terminal deletion. (**E**) Release probabilites (mean ± s.e.m.) derived from EPSC and sucrose pool estimates remained unchanged by the N-terminal deletions. (**F**) Recovery of the sucrose pool after depletion. (**G**) Recovery after train depletion was slowed down by N-terminal deletion. The quantity plotted is the amplitude of the test pulse (I_{test}) minus the amplitude of the last train EPSC (I_{last}), divided by the amplitude of the first train EPSC (I_{1st}) minus the amplitude of the last train EPSC (I_{last}). This is the recovery of the component, which disappears during a train. (**H**) Example spontaneous mEPSC traces in the presence of TTX. (**I**) mEPSC amplitudes. (**J**) mEPSC frequencies (mean ± s.e.m.) were increased for the NΔ24 mutant (**$P < 0.01$; ***$P < 0.001$).

Figure 6E). The effect magnitude of the middle mutations was moderate, though clearly distinguishable (Figure 6F), whereas the NΔ24 displayed a somewhat stronger effect (Figure 6G), and possibly a larger fraction of the fastest component.

These data indicate that the probability of releasing a vesicle increases mildly by mutations designed to destabilize the middle or N-terminal end of the complex. However, the mutations did not result in an increase in the fraction of the RRP$_{suc}$ released by a single action potential (Figures 4 and 5). This finding is puzzling, but might be explained if the mutations studied here preferentially affect the release of 'synchronous' vesicles, which consist of a sub-pool of the RRP$_{suc}$ vesicles released in the beginning of an AP train
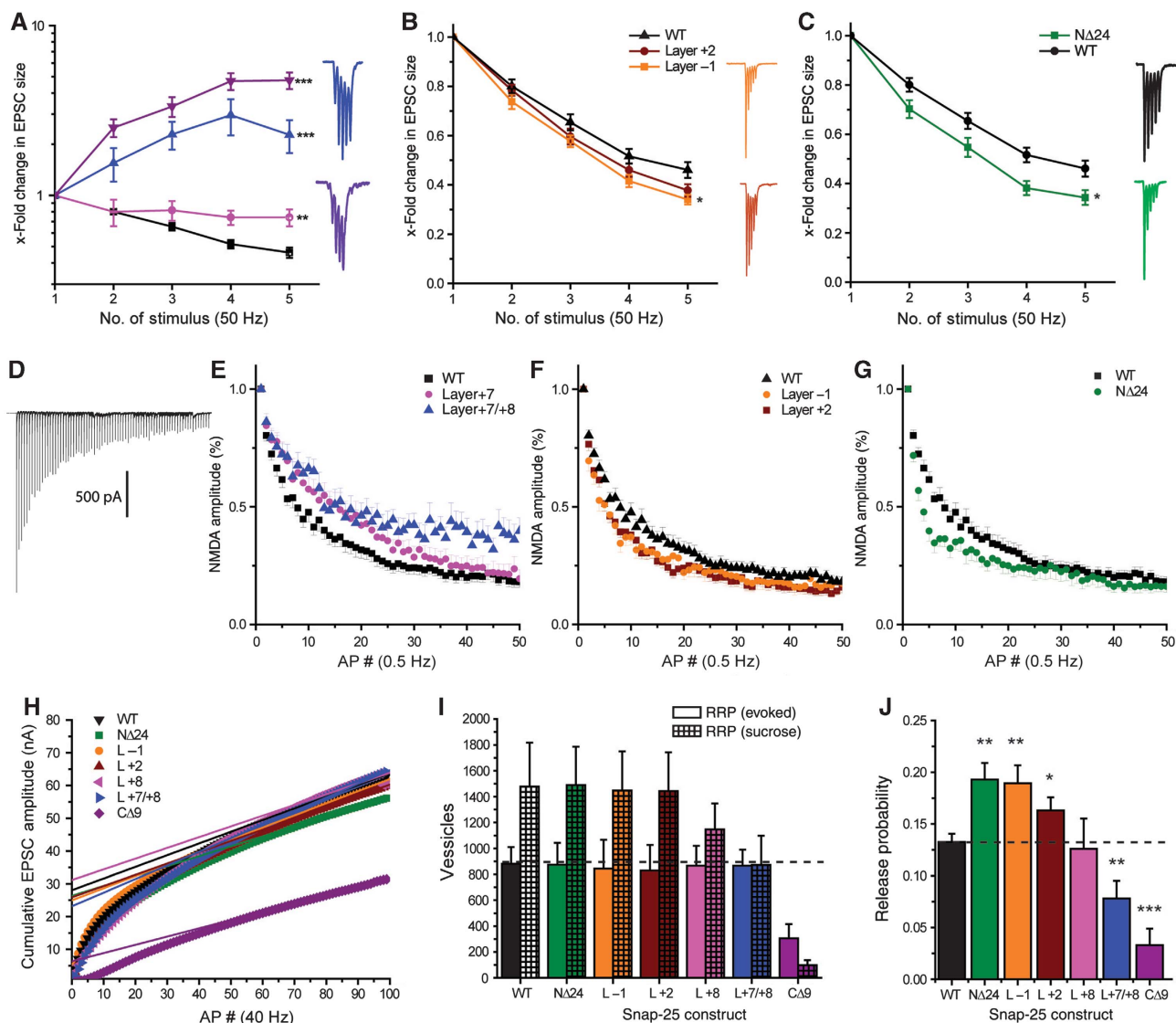
Figure 6 Mutations in the N-terminal part of the SNARE-motif increase and C-terminal mutations decrease vesicular release probabilities. (**A–C**) Short-term plasticity (five stimuli at 50 Hz; mean ± s.e.m.) with representative traces; EPSC amplitudes are normalized to the amplitude of the first EPSC. Colour coding according to Figure 1. (**A**) C-terminal mutations led to a progressive shift from depression towards facilitation. (**B**) Middle mutations led to a significant deepening of the depression. (**C**) The N-terminal deletion significantly increased depression. (**D–G**) Successive block of NMDA receptors with MK801. EPSCs driven by NMDA receptors are normalized to the amplitude after the first stimulation. (**D**) Example NMDA train in the presence of 5 μM MK801. (**E**) C-terminal mutations led to slower rundown of NMDA-EPSCs, indicative of a lower release probability. (**F**) Middle mutations led to a faster rundown of NMDA-EPSCs, indicative of a higher release probability. (**G**) The N-terminal deletion also led to faster rundown, indicative of a higher release probability. (**H–J**) RRP_{ev} and release probability estimates derived from AP trains. (**H**) Mean cumulative EPSC amplitudes plotted versus AP number including a steady-state line fit and back-extrapolation to time 0. Note that the quantities in (**I, J**) were calculated based on fits to individual experiments, not a fit to the mean data shown here. (**I**) RRP (mean ± s.e.m.) given in number of vesicles estimated with sucrose (RRP_{suc}) and train stimulation (RRP_{ev}). (**J**) Vesicular release probability (mean ± s.e.m.) derived from trains. C-terminal mutations caused a decrease, whereas more N-terminal mutations increased vesicular release probabilities (*$P<0.05$; **$P<0.01$; ***$P<0.001$).

(Moulder and Mennerick, 2005; Stevens and Williams, 2007) or by single APs (such as in MK801 experiments). We, therefore, alternatively estimated RRP size (denoted RRP_{ev}) by back-extrapolating a linear fit to the cumulative EPSC amplitudes measured during an AP train (100 APs, 40 Hz; Figure 6H) (Schneggenburger *et al*, 1999). This method resulted in a reduction of apparent RRP size by 40–50% (Figure 6I), in excellent agreement with an earlier report; see Figure 6C in Moulder and Mennerick (2005). The release probability of vesicles in the 'fast' sub-pool (RRP_{ev}) was now estimated by dividing the first EPSC amplitude of the train

with the pool estimate. This release probability was significantly increased for NΔ24, Layer −1 and Layer +2 mutations, whereas C-terminal mutations led to a progressive decrease (Figure 6J).

In conclusion, mutations in the C-terminal end of the SNARE-motif lead to a decreased release probability, whereas more N-terminal mutations increase release probability from the fastest sub-pool of the RRP_{suc}. Thus, similarly to data obtained on spontaneous release, mutations in the C- and N-terminal sub-domains of the SNARE-motif lead to opposite effects.

Train stimulation: changes in standing current and delayed release

We finally investigated the performance under high-use conditions. We separated the currents obtained during a 40-Hz train (100 APs) in EPSC amplitudes and standing currents (Figure 7A). The standing current originates from vesicles that fuse during the train, possibly with a contribution of glutamate 'spill-over', which might activate nearby receptors.

In wild-type-rescued neurons, the EPSCs decreased in size during the beginning of the train, whereas the standing current increased (Figure 7D–F). With C-terminal mutants, the train displayed more facilitation, as expected, but the

standing current nevertheless built up to levels indistinguishable from wild type, except in the CΔ9 (Figure 7F). This indicates that unless the destabilization to the C-terminal end becomes very pronounced, vesicles can still prime and fuse 'on the fly' during the train and is in good agreement with the unchanged size of the RRP$_{ev}$ found for C-terminal mutations (except the CΔ9) in Figure 6I. With the middle mutations, no major changes were noted (Figure 7E). The NΔ24 mutant displayed a decrease in standing current during the entire train, indicating that fewer vesicles were getting primed and fused during the train (Figure 7D). A final measurement was made of the 'delayed current', the current, which decays to
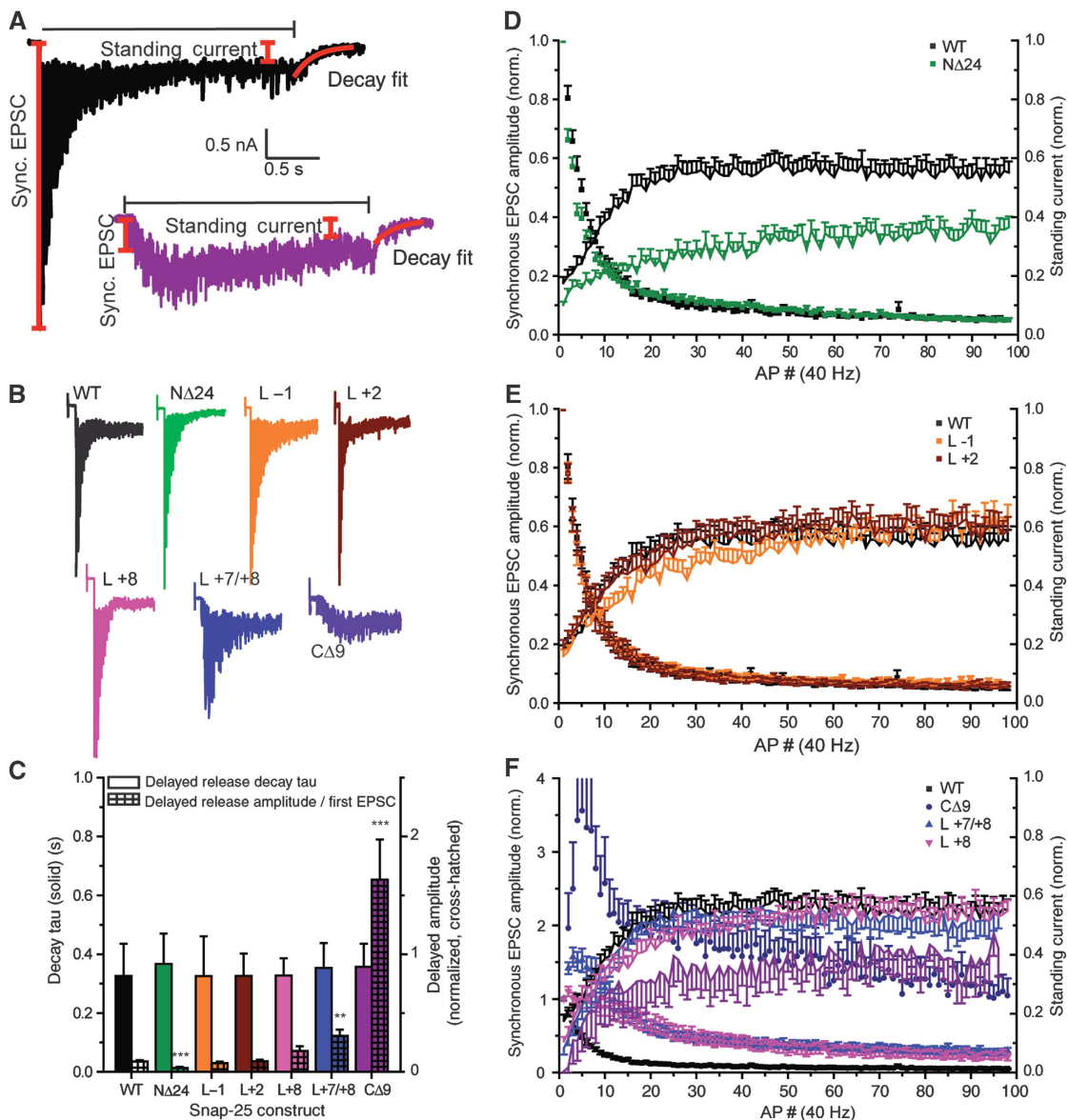
Figure 7 An N-terminal deletion delays priming and fusion of synaptic vesicles during train stimulation. (**A**) Example traces with measured values; the horizontal black line indicates duration of train stimulation, red lines show definition of first synchronous EPSC, standing current and fit of delayed current. (**B**) Example train stimulations for different mutants (colour coding according to Figure 1). (**C**) Amplitudes of the delayed current after train stimulation normalized to first EPSC amplitude (coloured cross-hatched bars) and time constant (τ) of the decay to baseline (coloured bars). The amplitude of the delayed current was significantly depressed by N-terminal deletion. (**D–F**) Depression of EPSC amplitudes during a train (symbols, left ordinates) and relative increase of standing current (lines, right ordinates). (**D**) The N-terminal deletion NΔ24 depressed the amplitude of the standing current. (**E**) Middle mutations did not significantly change the standing current. (**F**) C-terminal mutations led to progressive facilitation (as shown also in Figure 6), but delayed currents were intact except in the CΔ9 deletion, in which they fell behind (**$P<0.01$; ***$P<0.001$).

baseline as $[Ca^{2+}]_i$ relaxes after the train. In the NΔ24 mutant, the amplitude of the delayed current was depressed (Figure 7C). With the Layer −1 and Layer −2 mutations, no changes were observed, whereas in the C-terminal mutations, the delayed currents were increased. The latter finding was, however, not because of an increase in absolute current amplitude, but because of the normalization to the first EPSC amplitude (Figure 7C). None of the mutations changed the time constant of current relaxation to baseline (Figure 7C).

These data show that the delay in recovery of the EPSC found in the NΔ24 mutant (Figure 5G) correlates with a decrease in standing and delayed currents. In contrast, delayed and standing currents were quite resistant to C-terminal mutation, even when these mutations lead to severely impaired EPSC amplitude in response to single APs. These findings are consistent with the idea that N-terminal assembly of the SNARE-bundle underlies the vesicle priming reaction (which becomes rate limiting during trains), whereas C-terminal assembly is catalysed by calcium and drives the final triggering reaction (Sorensen *et al*, 2006).

Discussion

In this investigation, we have mutated the SNARE-complex from its N-terminal to its C-terminal end. The phenotypes of those mutations display clear region specificity, indicating that different parts of the SNARE-bundle have distinct functions during neurotransmission.

C-terminal mutations and the probability for release
Our data on three C-terminal mutations with increasing severity (Layer +8, Layer +7/+8 and C9) showed that the C-terminal end of the SNARE-complex is involved in setting the probability for both evoked and spontaneous release. The shift towards short-term synaptic facilitation by C-terminal mutation is consistent with data obtained after intoxication with BoNT/A (Capogna *et al*, 1997; Trudeau *et al*, 1998; Sakaba *et al*, 2005; Young, 2005), and also with a mutagenesis study, which used rescue of intoxicated cells with BoNT/E-insensitive SNAP-25 (Finley *et al*, 2002). These phenotypes also agree with the work in adrenal chromaffin cells, in which a decrease in maximal release rate and interference with the fusion pore were reported after C-terminal perturbation (Criado *et al*, 1999; Wei *et al*, 2000; Gil *et al*, 2002; Sorensen *et al*, 2006; Walter *et al*, 2010). The graded phenotypes caused by progressive mutations show that this effect most likely scales with the stability of the C-terminal end of the SNARE-complex.

The effect of C-terminal mutation was larger on spontaneous than on evoked release; for instance, whereas the triple mutations (Layer +7/+8) reduced the rate of spontaneous release to 3.3% of control values, the evoked release probability was only reduced to ∼25–35% (Figures 3E and 6J). In chromaffin cells (Sorensen *et al*, 2006), as well as in this study (Supplementary Figure 4), we could show that C-terminal destabilization changes the calcium dependence of exocytosis, or—put differently—calcium can help overcome the defect caused by C-terminal destabilization (Capogna *et al*, 1997; Trudeau *et al*, 1998; Sakaba *et al*, 2005). This finding indicates that calcium binding to synaptotagmin—the calcium sensor for exocytosis—is very likely energetically coupled to the assembly of the C-terminal end of the SNARE-complex, which in turn has a direct function in membrane fusion.

SNARE-complex and spontaneous neurotransmitter release
Data from knockout mice and flies showed that after elimination of SNAREs, evoked release was reduced more than spontaneous release (Deitcher *et al*, 1998; Schoch *et al*, 2001; Washbourne *et al*, 2002; Bronk *et al*, 2007; Delgado-Martinez *et al*, 2007; Maximov *et al*, 2009). Strikingly, our mutations in the C-terminal end of the SNARE-motif of SNAP-25 showed the opposite: spontaneous release rates suffered more than evoked release. These observations show that the structural requirements for spontaneous release at least involve a stable C-terminal end of the SNARE-complex. Interestingly, although spontaneous release is critically dependent on the C-terminal SNARE-layers, it is less dependent on the exact length of the synaptobrevin linker, which connects the SNARE-domain with the transmembrane anchor (Deak *et al*, 2006). This situation closely correlates with *in vitro* fusion assays (McNew *et al*, 1999; Siddiqui *et al*, 2007), indicating that those assays resemble spontaneous release.

In contrast to C-terminal mutations, mutations in the rest of the SNARE-motif caused an increased frequency of mEPSCs, indicating that the integrity of the N-terminal SNARE-bundle limits spontaneous release. Two non-exclusive explanations for this observation can be envisioned: either the destabilization of the SNARE-complex in itself favours spontaneous release, or the SNARE-complex has lost the ability to interact with auxiliary factors needed to limit spontaneous release. In some systems, deletion of complexin (Huntwork and Littleton, 2007; Maximov *et al*, 2009) or synaptotagmin-1 (Littleton *et al*, 1993; Pang *et al*, 2006; Kerr *et al*, 2008; Liu *et al*, 2009) causes an increase in spontaneous release rates, which has been explained by a 'clamp' function of those proteins, or—in the case of synaptotagmin—by the presence of other isoforms (Xu *et al*, 2009). However, in autaptic neurons—such as those used here—deletion of complexin or synaptotagmin apparently does not increase spontaneous release rates (Geppert *et al*, 1994; Reim *et al*, 2001; Xue *et al*, 2007; Liu *et al*, 2009). That our N-terminal mutants interact with synaptotagmin-1 and complexin to at least some extent is also indicated by the phenotypes of those mutants, which were neither desynchronized, as in the *synaptotagmin-1* null (Geppert *et al*, 1994), nor shifted in their calcium dependence as in the *complexin* null (Reim *et al*, 2001). Finally, we showed (Supplementary Figure 1) that our mutants still form SNARE-complexes and bind to complexin, even though we do not rule out that the interaction could be subtly changed (see below).

N-terminal end and priming of vesicles
The NΔ24 mutation delayed recovery of the EPSC amplitude after a train, and also decreased the standing and delayed currents on train stimulation, indicating that the N-terminal of the SNARE-complex is involved in vesicle priming under both conditions. Thus, initial N-terminal SNARE-complex association most likely underlies the vesicle priming step (Sorensen *et al*, 2006; Walter *et al*, 2010), even though the lower expression level of the NΔ24 mutant might affect this

conclusion. However, in adrenal chromaffin cells, but not in neurons, double alanine substitutions around the middle of the complex interfered with vesicle priming, resulting in smaller primed vesicle pools (Sorensen *et al*, 2006). Thus, vesicle priming seems to be more robust to SNARE-mutation in neurons, possibly because synaptic vesicle priming depends on a finite number of priming slots close to presynaptic calcium channels, whereas secretory vesicles in chromaffin cells can prime anywhere on the plasma membrane. This would tend to keep primed vesicle sizes more constant in neurons than in chromaffin cells.

It is incompletely understood how 'synchronous' and 'asynchronous' release phases contribute to the 'standing current' during a train in hippocampal neurons (see also Stevens and Williams, 2007). In the Calyx of Held synapse, a reluctant vesicle pool, which recovers fast after release, contributes significantly to release during trains, whereas single EPSCs are supported by a fast pool of vesicles (Sakaba and Neher, 2001; Sakaba, 2006). If these data can be translated to hippocampal neurons, assembly of the N-terminal end of the SNARE-complex underlies recovery of both vesicle pools.

Even though the recovery after an AP train was depressed in the NΔ24 mutant, recovery of the sucrose pool was normal. Similar data have been obtained after mutation of Munc18 and Munc13, two priming factors assumed to assist in SNARE-complex assembly (Junge *et al*, 2004; Wierda *et al*, 2007). After N-terminal deletion of SNAP-25, recovery after an AP train was almost as slow as recovery of the sucrose pool. This might indicate that NΔ24 specifically slows down a calcium-dependent recovery pathway, whereas an alternative and calcium-independent recovery path remains unaffected. However, as assembly of the SNARE-complex is necessary for all evoked release, another possibility is that sucrose application itself helps overcome the defect in the NΔ24 mutant, possibly by stimulating SNARE-complex assembly.
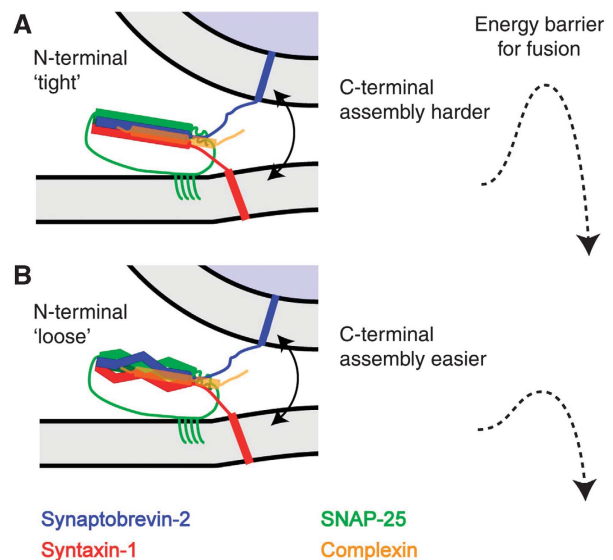
Two different SNARE-sub-domains with opposing effects on neurotransmission

Overall, our data show that mutations designed to compromise the SNARE-bundle affect neurotransmission in two different directions: whereas C-terminal mutations led to a decrease in the probability for evoked and spontaneous release, mutations in the rest of the bundle caused an increase in both parameters. In both cases, the spontaneous release rate was affected more than evoked release. The increase in evoked release probability was not seen when comparing the charge released by a single AP to the RRP size estimated by sucrose stimulation (RRP$_{suc}$), but it consistently showed up when the RRP size was estimated by a train of APs (RRP$_{ev}$) and in MK801 experiments. This discrepancy most likely indicates that the change only affects the fastest sub-pool of the RRP.

The opposing effects of C- and N-terminal or middle mutations imply that in a certain sense the two different parts of the SNARE-complex stimulate and inhibit release, respectively. At the same time, however, the SNARE-complex in its entirety is required for exocytosis. This is not as surprising, as it might seem at first sight. Several proteins, including complexin, synaptotagmin and Munc18-1, have been ascribed both positive and negative effects in neurotransmission (Sorensen, 2009). Indeed, both effects are

needed: the release machinery must not only trigger fast release, but also prevent release from taking place prematurely. It seems that the N-terminal part of the SNARE-complex is involved in both vesicle priming and limiting spontaneous release, whereas the C-terminal end is involved in driving membrane fusion forward.

What might the mechanism be for the inhibitory effect of the N-terminal part of the SNARE-complex on spontaneous release, and partly on evoked release? One possibility is that the activities of the two domains in the SNARE-complex are linked to each other: tight assembly of the N-terminal SNARE-bundle might put up an additional obstacle for the C-terminal end to assemble and trigger membrane fusion (Figure 8A), while at the same time linking C-terminal assembly to the activity of the calcium sensor, synaptotagmin. Conversely, if the N-terminal end is loosened, the C-terminal end might assemble more easily, triggering release (Figure 8B). This mechanism closely resembles the recent hypothesis on the action of complexin on the exocytosis complex. Data from various systems are consistent with the notion that the 'accessory helix' of complexin binds to the C-terminal end of the SNARE-complex *in lieu* of synaptobrevin-2, thereby clamping the SNARE-complex (Xue *et al*, 2007; Giraudo *et al*, 2009; Maximov *et al*, 2009). However, to put the accessory helix in the right position, complexin first has to bind around the middle of the SNARE-bundle through its central helix. This mechanism creates exactly the kind of interaction between N- and C-terminal sub-domains, which we assume here, and it is even possible that this mechanism underlies our findings. N-terminal or middle mutations might interfere with complexin binding and thereby with the ability of the accessory helix to stop premature C-terminal SNARE

Figure 8 A suggestion: two different sub-domains in the SNARE-complex have partly opposing functions for neurotransmitter release. (**A**) We here suggest that the tight assembly of the N-terminal two-thirds of the SNARE-complex puts up an additional obstacle for the C-terminal end to assemble and trigger membrane fusion, resulting in a higher barrier for fusion and less spontaneous release. Complexin might exacerbate this mechanism (see Discussion). (**B**) Conversely, if the N-terminal end is looser, assembly of the C-terminal end might become easier, resulting in a lower fusion barrier and more spontaneous fusion.

assembly and fusion. Our pull-down experiments did not identify impaired complexin binding to *cis*-SNARE-complexes (Supplementary Figure 1), but they also cannot rule out a small effect, as binding to *trans*-SNARE-complexes might have slightly different properties. Another possibility is that the interaction between N- and C-terminal domains is an intrinsic feature of the neuronal SNARE-complex, which is exacerbated or stabilized by the binding of complexin. This hypothesis would solve two additional problems. First, it might account for the mild increase in release probability of evoked release seen by N-terminal and middle mutations, which does not agree with the expectation from a lack of complexin binding. Second, it might explain how membrane fusion is stopped after the beginning of N-terminal SNARE-complex assembly. As complexin interacts mostly with synaptobrevin (Chen *et al*, 2002), it is hard to understand how it can succeed in blocking fusion, because it cannot bind until the SNARE-complex starts assembling. An internal brake in the SNARE-complex, which prevents C-terminal assembly, might be needed to allow complexin time to interact. The main testable prediction of this model is that the two ends of the SNARE-complex are coupled, such that the N-terminal domain affects the ease with which the C-terminal end assembles to trigger release.

Materials and methods

Cell culture
Astrocyte feeder islands and hippocampal neurons were prepared as described (Delgado-Martinez *et al*, 2007). Snap-25−/− embryos were obtained from heterozygous crossings at embryonic day 18 (E18). For electrophysiology, isolated hippocampal neurons were plated on astrocyte microislands (Bekkers and Stevens, 1991) in Neurobasal medium (Invitrogen, Carlsbad, CA) supplemented with B-27 (Invitrogen), 17.3 mM HEPES, 1% GlutaMax-I (Invitrogen), 1% penicillin/streptomycin (Invitrogen) and 25 μM β-mercaptoethanol. For immunocytochemistry, autaptic neurons were cultured on elaborated poly-D-lysine microdots. Neurons were cultured for 10–14 days before they were used for experiments. In both cases, only islands containing single neurons were examined. For cell survival and biochemical experiments, confluent astrocyte feeder layers with neurons plated at high density (50 k per coverslip) were used.

Lentiviral vectors
The lentivirus plasmid encoding SNAP-25B fused N-terminal to EGFP has been described before (Delgado-Martinez *et al*, 2007). A 25 amino-acid linker separates the EGFP from the complete SNAP-25B open reading frame. Most SNAP-25 mutations were earlier studied in chromaffin cells after introduction into the SNAP-25A isoform (Sorensen *et al*, 2006). Here, we introduced the mutations into SNAP-25B, the dominant SNAP-25 isoform in the hippocampus, by means of PCR mutagenesis. In addition, a mutant SNAP-25B lacking the first (N-terminal) 24 amino acids was constructed. All constructs were verified by sequencing. Lentiviruses were produced, aliquoted and frozen as described earlier (Delgado-Martinez *et al*, 2007). A total of 250 000 infectious units were added per neuronal culture at DIV 1.

Immunocytochemistry
Hippocampal neuronal cultures on poly-D-lysine-coated coverslips were fixed for 20 min at room temperature in PBS containing 4% paraformaldehyde. After three washes in PBS, fixed cells were incubated in PBS containing 0.1% Triton X-100, 10% goat serum and 2% BSA for 30 min to block non-specific binding. Cultures were incubated for 2 h with primary antibodies in the presence of goat serum (10%) and BSA (2%). Synapse count and branching analysis (Figure 2) were conducted using anti-synaptobrevin-2 (1:1000, mouse monoclonal, Synaptic Systems, Germany), and anti-MAP-2 (1:10 000, chicken polyclonal, Abcam) primary antibodies. For

testing colocalization between expressed constructs and synapses (Supplementary Figure 2), we used anti-synaptobrevin-2 (1:1000, mouse monoclonal, Synaptic Systems, Germany) and the intrinsic GFP-fluorescence of the EGFP-SNAP-25 constructs. The cells were washed three times with PBS and then incubated overnight with secondary antibodies: Alexa 546-coupled goat-anti-mouse (Invitrogen) and NL-637 anti-Chicken IgY (R&D Systems), both diluted 1:500 at 4°C. Immunofluorescence images were taken with a confocal microscope (LSM 410 controlled by LSM 3.98 software attached to an Axiovert 135TV (Figure 2) or LSM 510 META, LSM 4.2 SP1, Axiovert 200M (Supplementary Figure 2; Zeiss, Germany) using a 63 × oil immersion (1.4 NA) objective at 1024 × 1024 pixels. Images were imported into IgorPro (WaveMetrics) and the number of synapses and branching identified as described earlier (Delgado-Martinez *et al*, 2007).

Cosedimentation assays and western blotting
Cosedimentation assays were performed as described (Reim *et al*, 2005) with modifications. Recombinant fusion proteins consisting of GST alone or GST in frame with complexin (Cplx1) WT or Cplx1 K69A/Y70A (Xue *et al*, 2007) were expressed in *Escherichia coli* using pGEX-KG expression constructs. Recombinant proteins were purified on glutathion-agarose (Sigma), and immobilized on the resin for cosedimentation assays. Crude synaptosomes from mouse brains and protein extracts from neuronal cultures overexpressed with several SNAP-25 variants were solubilized at a protein concentration of 1 mg/ml in solubilization buffer containing 150 mM NaCl, 10 mM Hepes (pH 7.4), 1 mM EGTA, 2 mM MgCl$_2$, 1% (v/v) Triton X-100, 0.2 mM phenylmethylsulfonyl fluoride, 1 μg/ml aprotinin and 0.5 μg/ml leupeptin. To obtain enough protein from neuronal cultures for the experiments in Supplementary Figure 1, protein extracts from several preparations were combined. After stirring on ice for 10 min, insoluble material was removed by centrifugation (10 min at 346 000 g_{max} and 4°C). The equivalent of 0.5 mg of total protein was then incubated with 20 μg immobilized GST-fusion protein for 3 h at 4°C. Beads were then washed five times with solubilization buffer, resuspended in SDS–PAGE sample buffer, and analysed by SDS–PAGE and western blotting using standard procedures. Immunoreactive proteins were visualized with ECL (Amersham Biosciences) and semi-quantified using the integrated intensity of the signals with software NIH ImageJ 1.41o. The following primary antibodies were used for immunodetection: monoclonal antibodies to Syntaxin-1 (clone 78.2, 1:20 000), Synaptobrevin-2 (clone 69.1, 1:7500) and SNAP-25 (clone 71.1, 1:10^6, all from Synaptic System).

Electrophysiology
Autaptic cells between DIV 10 and 14 were used for experiments. The patch-pipette solution included 135 mM K-gluconate, 10 mM HEPES, 1 mM EGTA, 4.6 mM MgCl$_2$, 4 mM Na-ATP, 15 mM creatine phosphate and 50 U/ml phosphocreatine kinase, 300 mOsm, pH 7.3. The standard extracellular medium consisted of 140 mM NaCl, 2.4 mM KCl, 10 mM HEPES, 10 mM glucose, 4 mM CaCl$_2$ and 4 mM MgCl$_2$, 300 mOsm, pH 7.3. Cells were whole-cell voltage clamped at −70 mV with an EPC-9 amplifier (HEKA Elektronik, Lambrecht/Pfalz, Germany) under control of Pulse 8.80 software (HEKA Elektronik). Currents were low-pass filtered at 1 or 5 kHz and stored at either 10 or 20 kHz. Pipette resistance ranged from 4 to 6 MΩ. The series resistance was compensated for 75%. Only cells with series resistances below 20 MΩ were analysed. All recordings were made at room temperature. EPSCs were evoked by depolarizing the cell from −70 to 0 mV for 2 ms. Solutions were exchanged through a fast local multi-barrel perfusion system (Warner SF-77B, Warner Instruments). The patch pipettes were made of borosilicate glass and pulled using a multi-step puller (P-87; Sutter Instruments, Novato, CA). Successive NMDA blocking was performed according to Rosenmund *et al* (1993) and Xue *et al* (2007) in an extracellular solution containing 140 mM NaCl, 2.4 mM KCl, 10 mM HEPES, 10 mM glucose, 4 mM CaCl$_2$ and 10 μM glycine. Sucrose experiments were performed with 500 mM sucrose in tetrodotoxin (TTX, 500 nM) containing extracellular solution. Recording of miniature EPSCs (mEPSCs) was performed in the presence of 200 nM TTX. Spontaneous events were detected using Mini Analysis program (Synaptosoft). The calcium dose–response curve in Supplementary Figure 4 was recorded in extracellular solution containing 140 mM NaCl, 2.4 mM KCl, 10 mM HEPES, 10 mM glucose and 1 mM MgCl$_2$.

$CaCl_2$ was added from a 5M stock solution to reach concentrations from 1 to 12 mM.

Statistics

The results are shown as average $\pm$ s.e.m., with n (given in parenthesis) referring to the number of cells from each group unless otherwise indicated. When comparing two groups, the variances were first compared using an F-test. In case of homoscedastic data (F-test insignificant), we tested differences between group means using a Student's t-test. In case of heteroscedastic data (F-test significant), we tested difference between group medians using a Mann–Whitney U-test. Significance was assumed when $P < 0.05$. Statistical testing was performed using Origin Pro 8 (OriginLabs). In figures, the significance levels are indicated by asterisks; $*P < 0.05$; $**P < 0.01$; $***P < 0.001$.

Supplementary data

Supplementary data are available at *The EMBO Journal* Online (http://www.embojournal.org).

Conflict of interest

The authors declare that they have no conflict of interest.

References

Basu J, Betz A, Brose N, Rosenmund C (2007) Munc13-1 C1 domain activation lowers the energy barrier for synaptic vesicle fusion. *J Neurosci* **27:** 1200–1210

Baumert M, Maycox PR, Navone F, De Camilli P, Jahn R (1989) Synaptobrevin: an integral membrane protein of 18,000 daltons present in small synaptic vesicles of rat brain. *EMBO J* **8:** 379–384

Bekkers JM, Stevens CF (1991) Excitatory and inhibitory autaptic currents in isolated hippocampal neurons maintained in cell culture. *Proc Natl Acad Sci USA* **88:** 7834–7838

Bennett MK, Calakos N, Scheller RH (1992) Syntaxin: a synaptic protein implicated in docking of synaptic vesicles at presynaptic active zones. *Science* **257:** 255–259

Birks RI, Macintosh FC (1957) Acetylcholine metabolism at nerve-endings. *Br Med Bull* **13:** 157–161

Bronk P, Deak F, Wilson MC, Liu X, Sudhof TC, Kavalali ET (2007) Differential effects of SNAP-25 deletion on Ca2 + -dependent and Ca2 + -independent neurotransmission. *J Neurophysiol* **98:** 794–806

Capogna M, McKinney RA, O'Connor V, Gahwiler BH, Thompson SM (1997) Ca2 + or Sr2 + partially rescues synaptic transmission in hippocampal cultures treated with botulinum toxin A and C, but not tetanus toxin. *J Neurosci* **17:** 7190–7202

Chen X, Tomchick DR, Kovrigin E, Arac D, Machius M, Sudhof TC, Rizo J (2002) Three-dimensional structure of the complexin/SNARE complex. *Neuron* **33:** 397–409

Criado M, Gil A, Viniegra S, Gutierrez LM (1999) A single amino acid near the C terminus of the synaptosomeassociated protein of 25 kDa (SNAP-25) is essential for exocytosis in chromaffin cells. *Proc Natl Acad Sci USA* **96:** 7256–7261

de Wit H, Walter AM, Milosevic I, Gulyas-Kovacs A, Riedel D, Sorensen JB, Verhage M (2009) Synaptotagmin-1 docks secretory vesicles to syntaxin-1/SNAP-25 acceptor complexes. *Cell* **138:** 935–946

Deak F, Shin OH, Kavalali ET, Sudhof TC (2006) Structural determinants of synaptobrevin 2 function in synaptic vesicle fusion. *J Neurosci* **26:** 6668–6676

Deak F, Xu Y, Chang WP, Dulubova I, Khvotchev M, Liu X, Sudhof TC, Rizo J (2009) Munc18-1 binding to the neuronal SNARE complex controls synaptic vesicle priming. *J Cell Biol* **184:** 751–764

Deitcher DL, Ueda A, Stewart BA, Burgess RW, Kidokoro Y, Schwarz TL (1998) Distinct requirements for evoked and spontaneous release of neurotransmitter are revealed by mutations in the Drosophila gene neuronal-synaptobrevin. *J Neurosci* **18:** 2028–2039

Delgado-Martinez I, Nehring RB, Sorensen JB (2007) Differential abilities of SNAP-25 homologs to support neuronal function. *J Neurosci* **27:** 9380–9391

Elferink LA, Trimble WS, Scheller RH (1989) Two vesicle-associated membrane protein genes are differentially expressed in the rat central nervous system. *J Biol Chem* **264:** 11061–11064

Fasshauer D, Margittai M (2004) A transient N-terminal interaction of SNAP-25 and syntaxin nucleates SNARE assembly. *J Biol Chem* **279:** 7613–7621

Fasshauer D, Sutton RB, Brunger AT, Jahn R (1998) Conserved structural features of the synaptic fusion complex: SNARE proteins reclassified as Q- and R-SNAREs. *Proc Natl Acad Sci USA* **95:** 15781–15786

Finley MF, Patel SM, Madison DV, Scheller RH (2002) The core membrane fusion complex governs the probability of synaptic vesicle fusion but not transmitter release kinetics. *J Neurosci* **22:** 1266–1272

Geppert M, Goda Y, Hammer RE, Li C, Rosahl TW, Stevens CF, Sudhof TC (1994) Synaptotagmin I: a major Ca2 + sensor for transmitter release at a central synapse. *Cell* **79:** 717–727

Gil A, Gutierrez LM, Carrasco-Serrano C, Alonso MT, Viniegra S, Criado M (2002) Modifications in the C terminus of the synaptosome-associated protein of 25 kDa (SNAP-25) and in the complementary region of synaptobrevin affect the final steps of exocytosis. *J Biol Chem* **277:** 9904–9910

Giraudo CG, Garcia-Diaz A, Eng WS, Chen Y, Hendrickson WA, Melia TJ, Rothman JE (2009) Alternative zippering as an on-off switch for SNARE-mediated fusion. *Science* **323:** 512–516

Glitsch MD (2008) Spontaneous neurotransmitter release and Ca2 + —how spontaneous is spontaneous neurotransmitter release? *Cell Calcium* **43:** 9–15

Grosse G, Grosse J, Tapp R, Kuchinke J, Gorsleben M, Fetter I, Hohne-Zell B, Gratzl M, Bergmann M (1999) SNAP-25 requirement for dendritic growth of hippocampal neurons. *J Neurosci Res* **56:** 539–546

Hanson PI, Roth R, Morisaki H, Jahn R, Heuser JE (1997) Structure and conformational changes in NSF and its membrane receptor complexes visualized by quick-freeze/deep-etch electron microscopy. *Cell* **90:** 523–535

Hessler NA, Shirke AM, Malinow R (1993) The probability of transmitter release at a mammalian central synapse. *Nature* **366:** 569–572

Holt M, Varoqueaux F, Wiederhold K, Takamori S, Urlaub H, Fasshauer D, Jahn R (2006) Identification of SNAP-47, a novel Qbc-SNARE with ubiquitous expression. *J Biol Chem* **281:** 17076–17083

Huntwork S, Littleton JT (2007) A complexin fusion clamp regulates spontaneous neurotransmitter release and synaptic growth. *Nat Neurosci* **10:** 1235–1237

Jahn R, Scheller RH (2006) SNAREs—engines for membrane fusion. *Nat Rev Mol Cell Biol* **7:** 631–643

Junge HJ, Rhee JS, Jahn O, Varoqueaux F, Spiess J, Waxham MN, Rosenmund C, Brose N (2004) Calmodulin and Munc13 form a Ca2 + sensor/effector complex that controls short-term synaptic plasticity. *Cell* **118:** 389–401

Kerr AM, Reisinger E, Jonas P (2008) Differential dependence of phasic transmitter release on synaptotagmin 1 at GABAergic and glutamatergic hippocampal synapses. *Proc Natl Acad Sci USA* **105:** 15581–15586

Lan JY, Skeberdis VA, Jover T, Grooms SY, Lin Y, Araneda RC, Zheng X, Bennett MV, Zukin RS (2001) Protein kinase C modulates NMDA receptor trafficking and gating. *Nat Neurosci* **4:** 382–390

Littleton JT, Stern M, Schulze K, Perin M, Bellen HJ (1993) Mutational analysis of Drosophila synaptotagmin demonstrates its essential role in Ca(2 +)-activated neurotransmitter release. *Cell* **74:** 1125–1134

Liu H, Dean C, Arthur CP, Dong M, Chapman ER (2009) Autapses and networks of hippocampal neurons exhibit distinct synaptic transmission phenotypes in the absence of synaptotagmin I. *J Neurosci* **29:** 7395–7403

Lou X, Korogod N, Brose N, Schneggenburger R (2008) Phorbol esters modulate spontaneous and Ca2 + -evoked transmitter release via acting on both Munc13 and protein kinase C. *J Neurosci* **28:** 8257–8267

Maximov A, Tang J, Yang X, Pang ZP, Sudhof TC (2009) Complexin controls the force transfer from SNARE complexes to membranes in fusion. *Science* **323:** 516–521

McNew JA, Weber T, Engelman DM, Sollner TH, Rothman JE (1999) The length of the flexible SNAREpin juxtamembrane region is a critical determinant of SNARE-dependent fusion. *Mol Cell* **4:** 415–421

Moulder KL, Mennerick S (2005) Reluctant vesicles contribute to the total readily releasable pool in glutamatergic hippocampal neurons. *J Neurosci* **25:** 3842–3850

Oyler GA, Higgins GA, Hart RA, Battenberg E, Billingsley M, Bloom FE, Wilson MC (1989) The identification of a novel synaptosomal-associated protein, SNAP-25, differentially expressed by neuronal subpopulations. *J Cell Biol* **109:** 3039–3052

Pabst S, Margittai M, Vainius D, Langen R, Jahn R, Fasshauer D (2002) Rapid and selective binding to the synaptic SNARE complex suggests a modulatory role of complexins in neuroexocytosis. *J Biol Chem* **277:** 7838–7848

Pang ZP, Sun J, Rizo J, Maximov A, Sudhof TC (2006) Genetic analysis of synaptotagmin 2 in spontaneous and Ca2 + -triggered neurotransmitter release. *EMBO J* **25:** 2039–2050

Reim K, Mansour M, Varoqueaux F, McMahon HT, Sudhof TC, Brose N, Rosenmund C (2001) Complexins regulate a late step in Ca2 + -dependent neurotransmitter release. *Cell* **104:** 71–81

Reim K, Wegmeyer H, Brandstatter JH, Xue M, Rosenmund C, Dresbach T, Hofmann K, Brose N (2005) Structurally and functionally unique complexins at retinal ribbon synapses. *J Cell Biol* **169:** 669–680

Rizo J, Rosenmund C (2008) Synaptic vesicle fusion. *Nat Struct Mol Biol* **15:** 665–674

Rosenmund C, Clements JD, Westbrook GL (1993) Nonuniform probability of glutamate release at a hippocampal synapse. *Science* **262:** 754–757

Rosenmund C, Stevens CF (1996) Definition of the readily releasable pool of vesicles at hippocampal synapses. *Neuron* **16:** 1197–1207

Sakaba T (2006) Roles of the fast-releasing and the slowly releasing vesicles in synaptic transmission at the calyx of held. *J Neurosci* **26:** 5863–5871

Sakaba T, Neher E (2001) Calmodulin mediates rapid recruitment of fast-releasing synaptic vesicles at a calyx-type synapse. *Neuron* **32:** 1119–1131

Sakaba T, Stein A, Jahn R, Neher E (2005) Distinct kinetic changes in neurotransmitter release after SNARE protein cleavage. *Science* **309:** 491–494

Schneggenburger R, Meyer AC, Neher E (1999) Released fraction and total size of a pool of immediately available transmitter quanta at a calyx synapse. *Neuron* **23:** 399–409

Schoch S, Deak F, Konigstorfer A, Mozhayeva M, Sara Y, Sudhof TC, Kavalali ET (2001) SNARE function analyzed in synaptobrevin/VAMP knockout mice. *Science* **294:** 1117–1122

Selak S, Paternain AV, Aller MI, Pico E, Rivera R, Lerma J (2009) A role for SNAP25 in internalization of kainate receptors and synaptic plasticity. *Neuron* **63:** 357–371

Shen J, Tareste DC, Paumet F, Rothman JE, Melia TJ (2007) Selective activation of cognate SNAREpins by Sec1/Munc18 proteins. *Cell* **128:** 183–195

Siddiqui TJ, Vites O, Stein A, Heintzmann R, Jahn R, Fasshauer D (2007) Determinants of synaptobrevin regulation in membranes. *Mol Biol Cell* **18:** 2037–2046

Sorensen JB (2004) Formation, stabilisation and fusion of the readily releasable pool of secretory vesicles. *Pflugers Arch* **448:** 347–362

Sorensen JB (2009) Conflicting views on the membrane fusion machinery and the fusion pore. *Annu Rev Cell Dev Biol* **25:** 513–537

Sorensen JB, Wiederhold K, Muller EM, Milosevic I, Nagy G, de Groot BL, Grubmuller H, Fasshauer D (2006) Sequential N- to C-terminal SNARE complex assembly drives priming and fusion of secretory vesicles. *EMBO J* **25:** 955–966

Steegmaier M, Yang B, Yoo JS, Huang B, Shen M, Yu S, Luo Y, Scheller RH (1998) Three novel proteins of the syntaxin/SNAP-25 family. *J Biol Chem* **273:** 34171–34179

Stevens CF, Wesseling JF (1998) Activity-dependent modulation of the rate at which synaptic vesicles become available to undergo exocytosis. *Neuron* **21:** 415–424

Stevens CF, Williams JH (2007) Discharge of the readily releasable pool with action potentials at hippocampal synapses. *J Neurophysiol* **98:** 3221–3229

Sudhof TC, Rothman JE (2009) Membrane fusion: grappling with SNARE and SM proteins. *Science* **323:** 474–477

Sutton RB, Fasshauer D, Jahn R, Brunger AT (1998) Crystal structure of a SNARE complex involved in synaptic exocytosis at 2.4 A resolution. *Nature* **395:** 347–353

Tafoya LC, Mameli M, Miyashita T, Guzowski JF, Valenzuela CF, Wilson MC (2006) Expression and function of SNAP-25 as a universal SNARE component in GABAergic neurons. *J Neurosci* **26:** 7826–7838

Trudeau LE, Fang Y, Haydon PG (1998) Modulation of an early step in the secretory machinery in hippocampal nerve terminals. *Proc Natl Acad Sci USA* **95:** 7163–7168

Verderio C, Pozzi D, Pravettoni E, Inverardi F, Schenk U, Coco S, Proux-Gillardeaux V, Galli T, Rossetto O, Frassoni C, Matteoli M (2004) SNAP-25 modulation of calcium dynamics underlies differences in GABAergic and glutamatergic responsiveness to depolarization. *Neuron* **41:** 599–610

Voets T, Toonen RF, Brian EC, de Wit H, Moser T, Rettig J, Sudhof TC, Neher E, Verhage M (2001) Munc18-1 promotes large dense-core vesicle docking. *Neuron* **31:** 581–591

Walter AM, Wiederhold K, Bruns D, Fasshauer D, Sorensen JB (2010) Synaptobrevin N-terminally bound to syntaxin-SNAP-25 defines the primed vesicle state in regulated exocytosis. *J Cell Biol* **188:** 401–413

Wang LY, Kaczmarek LK (1998) High-frequency firing helps replenish the readily releasable pool of synaptic vesicles. *Nature* **394:** 384–388

Washbourne P, Thompson PM, Carta M, Costa ET, Mathews JR, Lopez-Bendito G, Molnar Z, Becher MW, Valenzuela CF, Partridge LD, Wilson MC (2002) Genetic ablation of the t-SNARE SNAP-25 distinguishes mechanisms of neuroexocytosis. *Nat Neurosci* **5:** 19–26

Wasser CR, Kavalali ET (2009) Leaky synapses: regulation of spontaneous neurotransmission in central synapses. *Neuroscience* **158:** 177–188

Wei S, Xu T, Ashery U, Kollewe A, Matti U, Antonin W, Rettig J, Neher E (2000) Exocytotic mechanism studied by truncated and zero layer mutants of the C-terminus of SNAP-25. *EMBO J* **19:** 1279–1289

Wierda KD, Toonen RF, de Wit H, Brussaard AB, Verhage M (2007) Interdependence of PKC-dependent and PKC-independent pathways for presynaptic plasticity. *Neuron* **54:** 275–290

Xu J, Pang ZP, Shin OH, Sudhof TC (2009) Synaptotagmin-1 functions as a Ca2 + sensor for spontaneous release. *Nat Neurosci* **12:** 759–766

Xue M, Reim K, Chen X, Chao HT, Deng H, Rizo J, Brose N, Rosenmund C (2007) Distinct domains of complexin I differentially regulate neurotransmitter release. *Nat Struct Mol Biol* **14:** 949–958

Young Jr SM (2005) Proteolysis of SNARE proteins alters facilitation and depression in a specific way. *Proc Natl Acad Sci USA* **102:** 2614–2619

Zucker RS, Regehr WG (2002) Short-term synaptic plasticity. *Annu Rev Physiol* **64:** 355–405